

CO₂-Stimulated Diversiform Deformations of Polymer Assemblies

Qiang Yan and Yue Zhao*

Département de Chimie, Université de Sherbrooke, Sherbrooke, Quebec J1K 2R1, Canada

S Supporting Information

ABSTRACT: Use of a given physiological stimulus to delicately deform polymer assemblies is a challenging topic. Here we develop synthetic block copolymers to construct a series of CO₂-sensitive self-assembled nanostructures that can simulate controllable deformations of the organelles in different ways. By controlling the CO₂ stimulation levels, one can modulate the size, shape, and morphology of the polymer aggregates, which is conducive to understanding the stimuli-triggered dynamic reshaping process of polymer assemblies in aqueous solution.

As one of the most inherent characteristics and intriguing abilities of living organisms, the shape changes of organelles under physiological stimuli are keys to executing biological functions and maintaining cell vitality.¹ For instance, several organelles show autonomous motions such as volume tuning, unfolding, and endocytosis (Scheme 1a).² Considering the componential multiplicity and the self-organized sophistication of the organelles, mimicking their stimuli-feedback

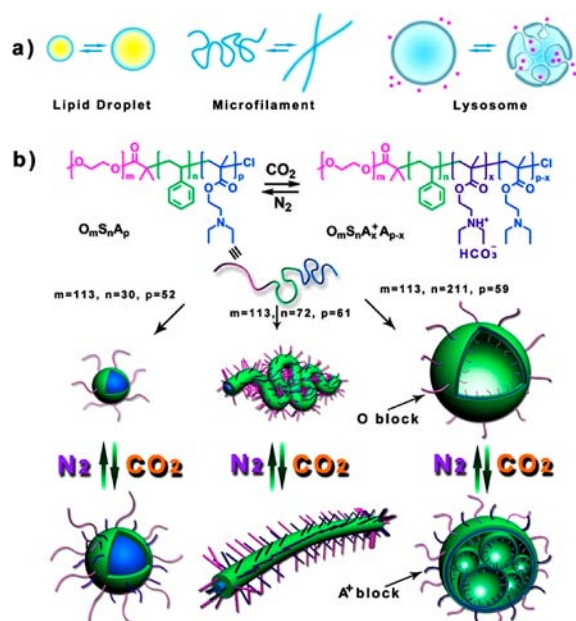
deformable behaviors by use of synthetic molecules has become a long-term goal in chemistry.³ As a class of macro-building blocks, block copolymers have spurred much interest since they can self-assemble into diversiform structures in aqueous solution, which makes them candidates for simulating organelle deformation.⁴ In this aspect, some successful studies have proven that the geometry of polymer assemblies can be transformed by fluctuating external conditions (i.e., pH, temperature, light, redox, and shear force).^{5–9}

Carbon dioxide, a pivotal endogenous metabolite, can penetrate across the protoplasmic membranes and play a crucial role in tuning the bilayer structure. Hence, exploiting CO₂ as a stimulus to subtly regulate the shape and property of polymer assemblies might hold great promise for organelle mimicry. Recently, some nascent efforts have been devoted to constructing CO₂-sensitive polymers,¹⁰ and some reports have shown that CO₂ can be used to modulate the shape of assemblies by tuning the protonation degree of the polymer chain.^{10a,b} We report success in utilizing CO₂ to stimulate deformations of block copolymer aggregates in different ways that mimic those of the organelles in Scheme 1a.

To realize that aim, we designed and synthesized a series of triblock copolymers, composed of outer hydrophilic poly(ethylene oxide) (termed O), middle hydrophobic poly(styrene) bridging block (S), and CO₂-responsive interior poly((2-diethylamino)ethyl methacrylate) flank (A) (O_mS_nA_p); for details of synthesis and characterization see the Supporting Information).¹¹ Having the same O block and a similar A block with varying lengths of the S bridge, OSA copolymers self-assemble into three initial nanostructures: spherical micelles, worm-like micelles, and vesicles, in all of which the A blocks constitute the inner part of the cores. By introducing CO₂ into the solution, the A blocks can be gradually protonated and changed to charged polyelectrolyte chains. However, since the A chains are enclosed by the hydrophobic S chains, the former can only undergo hydration confined by the latter. We speculated that such restricted hydration of the core chains and the repulsive interactions of charged polyelectrolyte chains might create a driving force to reshape the aggregated structures in a way realizing the automatic regulation (Scheme 1b).

Measurements first confirmed the CO₂-responsiveness of the OSA copolymers. Typically, we used the nanoprecipitation method to prepare the polymer solution. OSA was first dissolved in THF (1.2 mg/mL), a good solvent to all blocks. Deionized water was then injected at a slow rate (0.5 mL/h) to yield a translucent colloidal solution (THF/H₂O, 2/1, w/w),

Scheme 1. (a) Schematic of the Shape Regulation of Different Organelles; (b) CO₂-Switchable Triblock Copolymer OSA and Their CO₂-Driven Controlled Deformation for Biomimicking the Organellar Shape Regulation



Received: August 21, 2013

Published: October 24, 2013

and the organic phase was finally removed by dialysis. A strong Tyndall effect implies the formation of micellar particles. Their gas-sensitivity was examined by conductivity measurement.¹² As seen from the $O_{113}S_{30}A_{52}$ in Figure 1a, when CO_2 was

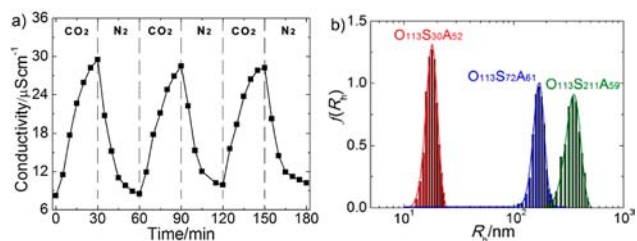


Figure 1. (a) Conductivity change of the $O_{113}S_{30}A_{52}$ copolymer in aqueous solution plotted versus time with alternating CO_2/N_2 stimulation. (b) DLS data for different OSA aggregates in the absence of stimulus.

passed through the polymer solution for 30 min, the conductivity increased rapidly from 8.2 to 29.5 $\mu S/cm$, accompanied by pH decrease from 7.20 to 5.86, as a result of the extra positive charge on copolymer chains owing to the protonation of the A blocks. Subsequently, by passing nitrogen through the solution to remove CO_2 , the conductivity was restored due to deprotonation. Repeatable cycles under an alternating CO_2/N_2 stimulation ensured the gas-responsive reversibility. Next, we explored whether different OSAs can self-assemble into different dimensional and morphological objects. With the used samples (Table S1), the aggregated size should only depend on the S segment. In general, the longer the hydrophobic S chain, the stronger the core-chain interaction, and thus the larger aggregates formed.¹³ To elucidate this point, dynamic light scattering (DLS) was employed to monitor the sizes of these polymer aggregates. As expected, with increasing the polymerization degree of S block from 30 through 72 to 211, the average hydrodynamic radius, R_h , accordingly rose from 18 through 175 to 360 nm, indicating the formation of distinct nanostructures (Figure 1b). In addition, a drop of the solution transmittance (78% \rightarrow 29%, Figure S4) with the S chain extension supported the size changes.

To visualize the size and morphological differences of the assemblies from the three OSA copolymers and further to verify whether they can deform through CO_2 stimulation, we used transmission electron microscopy (TEM) to track their deformable processes. For the $O_{113}S_{30}A_{52}$, without any stimulus, the copolymer can form typical spherical micelles (Figure 2a). Determined by TEM (averaged over 100 objects), the diameter ($D_{TEM} \approx D_{S-layer} + D_{A-layer}$) of the aggregates is 24 nm (Figure S5). The discrepancy between TEM and DLS results can be explained by the fact that DLS takes into account the length of the O layer while TEM, using dried samples, does not. These spherical nanoparticles were stable and kept in shape over three weeks if no stimulus was applied. But interestingly, CO_2 can activate them to begin an unexpected transition. After CO_2 bubbling for 10 min, they expanded to 142% of the initial size with a nearly uniform D_{TEM} of 34 nm (Figure 2b). Furthermore, the contrast between the dark center and the gray periphery suggests that the initial hydrophobic core comprising both the S and A blocks was divided into a core-shell structure upon hydration of the A block, in which the S chains form the shell layer that surrounds the A core. On

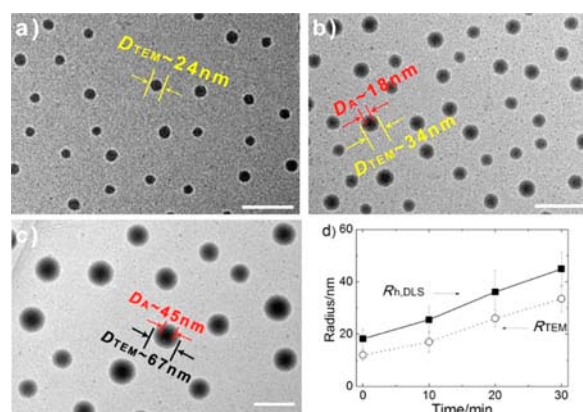


Figure 2. TEM images of $O_{113}S_{30}A_{52}$ aggregates at different levels of CO_2 stimulation for spherical micellar growth: (a) no stimulus, (b) 10 min, and (c) 30 min (scale bars: 100 nm). (d) Change in the radius of the aggregates from DLS and TEM results.

average, the size of the A core (D_A) is 18 nm and the thickness of the S shell (D_S) is 8 nm [$D_S = (D_{TEM} - D_A)/2$]. When we prolonged CO_2 aeration time to 30 min, the spheres further expanded to 67 nm in diameter, that is, nearly 280% of the initial size, while the thicknesses of the core and the shell layer increased to 45 and 11 nm, respectively (Figure 2c). The evolution of the particle size over the duration of the gas treatment was determined by using both DLS and TEM. The size increase proceeds in an almost linear fashion over CO_2 stimulation time (Figure 2d). It is worth noting that upon passage of N_2 in the solution, the size of the spheres can be reverted to the initial level (Figure S6). A control experiment revealed that nonacidic gas such as air is unable to activate the sphere growth (Figure S7). The entire process can be viewed as a micellar “breathing” movement,¹⁴ analogous to the organelle volume self-adjusting.

In the case of $O_{113}S_{72}A_{61}$, owing to its longer S block, the copolymer can spontaneously form one-dimensional worm-like nanostructures. They have a large length/diameter ratio: the D_{TEM} is ~ 28 nm, and the length reaches several micrometers, which is consistent with the equivalent radius of 175 nm from DLS. A great number of curving and curling sites in these nanofibers show their favorable crimpness (Figure 3a). While

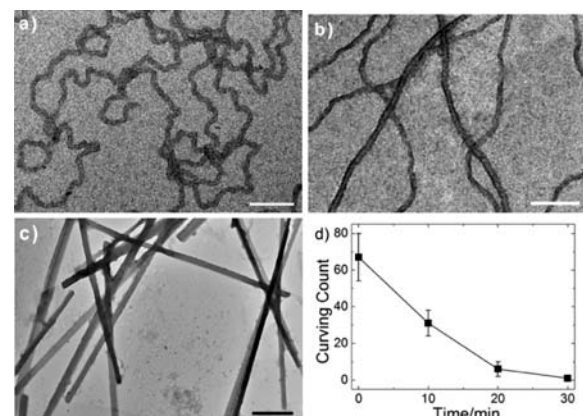


Figure 3. TEM images of $O_{113}S_{72}A_{61}$ aggregates at different levels of CO_2 stimulation with gas-tunable straightness: (a) no stimulus, (b) 15 min, and (c) 30 min (scale bars: 150 nm). (d) Average number statistics of the curly points in per nanofiber.

the microfilament can switch from curly to stretching status when given a biostimulus, our polymer fibrous analogues own the similar function under CO₂ stimulation. Upon CO₂ trigger for 15 min, the initial highly curly and folded fibrous aggregates started to be straightened and the crimpness had a notable decrease (Figure 3b). Continuously purging with CO₂ to 30 min, the flexible nanofibers completely converted to rigid straight nanowires, accompanied by a radial extension (D_{TEM} from 28 to 34 nm in Figure 3c). Counting the average curving sites in per fiber (estimated from ~ 30 objects) shows the unbending deformation with increasing the CO₂ level (Figure 3d). Upon alternating CO₂/N₂ stimulation, these cylinders can reversibly straighten and curl (Figure S8), which is in many ways reminiscent of the elastic telescopic motion of microfilaments.

The above results have revealed that depending on the length of the hydrophobic S block, CO₂ can tune the shape of OSA aggregates in different manners. Then what happens for the copolymer aggregates with the longest S block, O₁₁₃S₂₁₁A₅₉?

The phenomenon is equally striking. The copolymers first self-assembled into typical vesicles with the average D_{TEM} of 610 nm (close to the DLS analysis, Figure 4a). After the

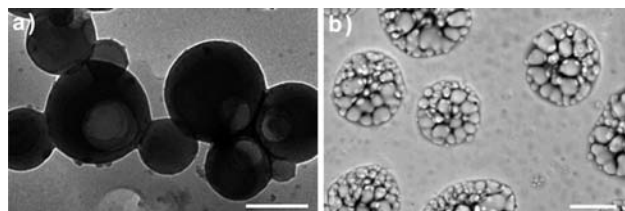


Figure 4. CO₂-driven O₁₁₃S₂₁₁A₅₉ vesicular shape transformation as monitored by TEM: (a) no stimulus and (b) gas-triggered 30 min (scale bars: 500 nm).

polymer solution was treated with CO₂ for 30 min, a shape shift appeared: large-compound sacs (LCSs) began to dominate in the solution.¹⁵ From the TEM image, it appears that each giant sac (ca. 610 nm) is compartmentalized into dozens of smaller irregular vacuoles (ranging from 40 to 180 nm) and a continuous membrane separates these vacuoles (Figure 4b). This morphological transition was also reversible upon alternating CO₂/N₂ stimulation. Such CO₂-triggered deformation of vesicles looks like, to some extent, the lysosomes' endocytosis behavior. The relationships between CO₂ aeration amount, solution pH, and the size/shape/morphology transformation of all three OSA aggregates are quantitatively summarized in Table S2.

Before discussing the possible shape transformation mechanism, we attempt to understand why different OSAs assemble into different initial structures. In general, the geometry of block copolymer amphiphiles can be predicted on the hydrophilic volume fraction (f_{philic}).¹⁶ Theoretically, spherical micelles should be formed when $f_{\text{philic}} > 50\%$, worm-like micelles when $40\% < f_{\text{philic}} < 50\%$, and vesicle/lamellar structure for $f_{\text{philic}} < 40\%$. For our OSA samples, by increasing the S block, the calculated f_{philic} decreases from 48% (O₁₁₃S₃₀A₅₂) through 34% (O₁₁₃S₇₂A₆₁) to 17% (O₁₁₃S₂₁₁A₅₉), corresponding to the formation of the globular, fibrous and vesicular aggregates, respectively (Table S3). The slight deviation between the actual and theoretical values is probably attributed to the stronger hydration effect of the charged A block than a noncharged hydrophilic block like O.

What follows is a proposed mechanism on how CO₂ drives the assemblies shape regulation. Considering the block copolymer structure, all the aggregates should have a layered structure, in which the hydrophilic O block acts as the outermost corona, the CO₂-responsive A chains serve as the inner core, and sandwiched between them is the hydrophobic S shell. The different CO₂-stimulated deformations of the OSA aggregates might be caused by effects of corona-chain charge repulsion and core-chain restricted hydration. In the absence of CO₂, the majority of A chains in the core are in deprotonated state. However, in the presence of CO₂, they become increasingly protonated and convert to the A⁺ species. Upon hydration of the A block (absorption of water), because the A core is surrounded by the hydrophobic S shell, the polyelectrolyte chains cannot dissolve freely; consequently, the hydration as well as the electrostatic repulsion among the charged A⁺ chains should result in an expansion of the core region. As the A core swelling develops with increasing the protonation degree of A chains, the S shell no longer has enough constraint to confine the core; part of charged A⁺ chains crack the barrier of S layer and extrude out of the core,¹⁴ forming a new corona with the hydrophilic O block. The charge repulsive interactions among A⁺ chains in the corona result in an increase of the interfacial free energy, which may drive the aggregates to shift their shape, so as to counterbalance the increasing free energy. For the spheres, the effect appears straightforward: CO₂ induces an abrupt increase of the A block protonation degree (0.38 \rightarrow 0.93), as a result, the uptake of water by the A⁺ chains within the sphere core and the repulsion of the A⁺ chains in the corona leads to the expansion of the aggregate. In the case of worm-like micelles, the restricted hydration of the A⁺ chains (protonated degree 0.29 \rightarrow 0.61) may cause a radial size expansion of the nanofibers (Figure 3) and create an internal pressure due to the water uptake. Moreover, the charge repulsion may result in stretching of the A⁺ chains that, being linked to the S chains in a random coil conformation, could act with the hydration effect to unfold the curly sections and give rise to straight nanowires. By contrast, the deformation of the vesicle into compartmentalized LCS is more intriguing. It seems that the confined expansion of the A layer upon hydration and charge repulsion could build up an internal stress and interfacial tension that push the membrane to deform in order to minimize the interfacial free energy.

A variety of experimental evidence supported the above mechanism. First is the change in the surface charge of the assemblies: before and after CO₂ was injected, the zeta potential of the OSA aggregates greatly increased from -4.8 to $+22.9$ mV (sphere), $+7.5$ to $+26.6$ mV (fiber), and $+5.2$ to $+21.2$ mV (vesicle), respectively (Figure S9). This indicates that part of the protonated A⁺ chains indeed form a new corona with positive charge. The second indication is the change of f_{philic} : upon CO₂ stimulation, although the f_{philic} has significant increase from 48% to 77% (sphere), 34% to 49% (fiber), and 17% to 32% (vesicle), respectively, they are still in the phase region of spherical, cylindrical and lamellar structure. This explains why the deformed assemblies can maintain their essential geometries. Third, we carried out a control experiment to verify the role of restricted hydration in the deformation process. We synthesized a block copolymer counterpart, O₁₁₃A₄₆S₆₁, differing from the OSA polymers by interchanging the positions of A and S. Similarly, this copolymer can assemble into spherical micelles. However, owing to the A block at the outer layer of the hydrophobic S block, upon CO₂ stimulation

the hydration and the A⁺ chains stretching are no longer subjected to the restriction of the S block. Even though stretching of the polyelectrolyte chains due to charge repulsion may occur at the interface, no expansion like the O₁₁₃S₃₀A₅₂ micelles was observed (Figure S10). This result points out the importance of having the hydration of the A block impeded by the hydrophobic S shell in inducing CO₂-stimulated deformations of the OSA assemblies. We mention that all samples for TEM were prepared by freeze-drying. Under this condition, the removal of water from hydrated polymer aggregates should affect little the observed size and morphology of the aggregates.

In conclusion, we have successfully exploited the use of CO₂ to stimulate deformations of polymer assemblies in ways that mimic the shape regulation of organelles. Using CO₂-responsive triblock copolymer of various compositions, diversiform gas-controlled deformations were realized: volume expansion of nanospheres, stretching of curly nanofibers, and compartmentalization of vesicles. Our study shows that the synergy of corona-chain repulsion and core-chain restricted hydration is an effective principle for stimuli-regulated deformation of block copolymer assemblies. It is expected that this method, combined with the polymer model, might offer new possibilities for biomimicking.

■ ASSOCIATED CONTENT

Supporting Information

Details of synthesis, UV-vis spectra, TEM statistics and images, SEM, DLS, and zeta potential analysis. This material is available free of charge via the Internet at <http://pubs.acs.org>.

■ AUTHOR INFORMATION

Corresponding Author

yue.zhao@usherbrooke.ca

Notes

The authors declare no competing financial interest.

■ ACKNOWLEDGMENTS

This work was financially supported by the Natural Sciences and Engineering Research Council of Canada (NSERC) and le Fonds de recherche du Québec: Nature et technologies (FRQNT). Y.Z. is a member of the FRQNT-funded Center for Self-Assembled Chemical Structures (CSACS) and the Centre québécois sur les matériaux fonctionnels (CQMF).

■ REFERENCES

- (1) (a) Kachar, B.; Bridgman, P. C.; Reese, T. S. *J. Cell. Biol.* **1987**, *105*, 1267–1271. (b) Di Paolo, G.; De Camilli, P. *Nature* **2006**, *443*, 651–657.
- (2) (a) Suzuki, M.; Shinohara, Y.; Ohsaki, Y.; Fujimoto, Y. *J. Electron Microsc.* **2011**, *60*, S101–S116. (b) Dickinson, R. B.; Caro, L.; Purich, D. L. *Biophys. J.* **2004**, *87*, 2838–2854. (c) Gruenberg, J. *Nat. Rev. Mol. Cell Biol.* **2001**, *2*, 721–730.
- (3) (a) Farsad, K.; De Camilli, P. *Curr. Opin. Cell Biol.* **2003**, *15*, 372–381. (b) Zhou, Y. F.; Yan, D. Y. *Angew. Chem., Int. Ed.* **2005**, *44*, 3223–3226. (c) Wilson, D. A.; Nolte, R. J. M.; van Hest, J. C. M. *Nat. Chem.* **2012**, *4*, 268–274. (d) Kim, K. T.; Zhu, J. H.; Meeuwissen, S. A.; Cornelissen, J. J. L. M.; Pochan, D. J.; Nolte, R. J. M.; van Hest, J. C. M. *J. Am. Chem. Soc.* **2010**, *122*, 12522–12524.
- (4) (a) Peters, R. J. R. W.; Louzao, I.; van Hest, J. C. M. *Chem. Sci.* **2013**, *3*, 335–342. (b) Pasparakis, G.; Krasnogor, N.; Cronin, L.; Davis, B. G.; Alexander, C. *Chem. Soc. Rev.* **2010**, *39*, 286–300. (c) Marguet, M.; Bonduelle, C.; Lecommandoux, S. *Chem. Soc. Rev.* **2013**, *42*, 512–529.

- (5) (a) Du, J. Z.; Armes, S. P. *J. Am. Chem. Soc.* **2005**, *127*, 12800–12801. (b) Rodriguez-Hernandez, J.; Lecommandoux, S. *J. Am. Chem. Soc.* **2005**, *127*, 2026–2027. (c) Doncom, K. E. B.; Hansell, C. F.; Theato, P.; O'Reilly, R. K. *Polym. Chem.* **2012**, *3*, 3007–3015.
- (6) (a) Pietsch, C.; Mansfeld, U.; Guerrero-Sanchez, C.; Hoepfner, S.; Vollrath, A.; Wagner, M.; Hoogenboom, R.; Sauben, S.; Thang, S. H.; Remzi Becer, C.; Chiefan, J.; Schubert, U. S. *Macromolecules* **2012**, *45*, 9292–9302. (b) Cai, Y.; Aubrecht, K. B.; Grubbs, R. B. *J. Am. Chem. Soc.* **2011**, *133*, 1058–1065. (c) Li, Y. T.; Lokitz, B. S.; McCormick, C. L. *Angew. Chem., Int. Ed.* **2006**, *45*, 5792–5795. (d) Hocine, S.; Brulet, A.; Jia, L.; Yang, J.; Cicco, A. D.; Bouteiller, L.; Li, M. H. *Soft Matter* **2011**, *7*, 2613–2623. (e) Moughton, A. O.; Patterson, J. P.; O'Reilly, R. K. *Chem. Commun.* **2011**, *47*, 355–357.
- (7) (a) Nalluri, S. K. M.; Ravoo, B. J. *Angew. Chem., Int. Ed.* **2010**, *49*, 5371–5374. (b) Jiang, J. Q.; Tong, X.; Zhao, Y. *J. Am. Chem. Soc.* **2005**, *127*, 8290–8291.
- (8) (a) Kim, H.; Jeong, S.-M.; Park, J.-W. *J. Am. Chem. Soc.* **2011**, *133*, 5206–5209. (b) Ryu, J. H.; Roy, R.; Ventura, J.; Thayumanavan, S. *Langmuir* **2010**, *26*, 7086–7092. (c) Power-Brillard, K. N.; Spontak, R. J.; Manners, I. *Angew. Chem., Int. Ed.* **2004**, *43*, 1260–1263.
- (9) Wang, C.-W.; Sinto, D.; Moffitt, M. G. *ACS Nano* **2013**, *7*, 1424–1436.
- (10) (a) Yan, Q.; Zhou, R.; Fu, C. K.; Zhang, H. J.; Yin, Y. W.; Yuan, J. Y. *Angew. Chem., Int. Ed.* **2011**, *50*, 4923–4927. (b) Yan, Q.; Zhao, Y. *Angew. Chem., Int. Ed.* **2013**, *52*, 9948–9951. (c) Yan, B.; Han, D.; Boissiere, O.; Ayotte, P.; Zhao, Y. *Soft Matter* **2013**, *9*, 2011–2016. (d) Zhou, K.; Li, J.; Lu, Y.; Zhang, G.; Xie, Z.; Wu, C. *Macromolecules* **2009**, *42*, 7146–7154. (e) Guo, Z.; Feng, Y.; Wang, Y.; Wang, J.; Wu, Y.; Zhang, Y. *Chem. Commun.* **2011**, *47*, 9348–9350. (f) Satav, S.; Bhat, S.; Thayumanavan, S. *Biomacromolecules* **2010**, *11*, 1735–1740. (g) Lin, S.; Theato, P. *Macromol. Rapid Commun.* **2013**, *34*, 1118–1133.
- (11) Han, D.; Tong, X.; Boissiere, O.; Zhao, Y. *ACS Macro Lett.* **2012**, *1*, 57–61.
- (12) Liu, Y. X.; Jessop, P. G.; Cunningham, M.; Eckert, C. A.; Liotta, C. L. *Science* **2006**, *313*, 958–960.
- (13) (a) Shen, H. W.; Eisenberg, A. *Macromolecules* **2000**, *33*, 2561–2572. (b) Azzam, T.; Eisenberg, A. *Angew. Chem., Int. Ed.* **2006**, *45*, 7443–7447.
- (14) Yu, S. Y.; Azzam, T.; Rouiller, I.; Eisenberg, A. *J. Am. Chem. Soc.* **2009**, *131*, 10557–10566.
- (15) Mai, Y. Y.; Zhou, Y. F.; Yan, D. Y. *Small* **2007**, *3*, 1170–1173. (b) Du, J. Z.; Chen, Y. M. *Angew. Chem., Int. Ed.* **2004**, *43*, 5084–5087.
- (16) Discher, B. M.; Won, Y.-Y.; Ege, D. S.; Lee, J. C.-M.; Bates, F. S.; Discher, D. E.; Hammer, D. A. *Science* **1999**, *284*, 1143–1146.